Contribution from the Department of Energy and Environment, Brookhaven National Laboratory, Upton, New York 11973

Reaction of Hydrogen with the Low-Temperature Form (C15) of $TiCr_2$

JOHN R. JOHNSON* and JAMES J. REILLY

Received March 24, 1978

At −78 °C the low-temperature form (C15) of the intermetallic compound $TiCr_2$ will react directly and reversibly with hydrogen to form two nonstoichiometric hydrides having the nominal compositions of $TiCr_{1.8}H_{2.6}$ and $TiCr_{1.8}H_{3.6}$. Both hydride phases are very unstable having, at −78 °C, dissociation pressures of ~2 and ~50 atm, respectively. Relative partial molal quantities for the formation of both hydrides are given. At room temperature, X-ray diffraction data indicate the existence of only one, highly nonstoichiometric hydride, $TiCr_{1.8}H_x$, where $2.1 < x < 3.6$. This phase is orthorhombic with the lattice parameters varying slightly with hydrogen content. For a composition corresponding to $TiCr_{1.8}H_{3.42}$, $a = 7.30$, $b = 5.18$, and $c = 4.94$ Å.

Introduction

Certain metal hydrides have been recognized for several years as potentially important energy storage compounds.[1] In the course of our work concerned with both fundamental and practical aspects of such materials, we have examined the reaction of hydrogen with Ti–Cr alloys. The phase diagram of this system, as determined by Farrar and Margolin,[2] is shown in Figure 1. It contains one intermetallic compound, having the nominal composition $TiCr_2$, of which there are two allotropes. Both allotropes are Laves phases, a low-temperature form having the cubic $MgCu_2$ (C15) structure which undergoes a transition to the hexagonal $MgZn_2$ (C14) structure at ~1000 °C. This paper will be concerned with the reaction of hydrogen with the cubic C15 phase and the formation and properties of two nonstoichiometric hydrides having the approximate compositions of $TiCr_2H_{2.6}$ and $TiCr_2H_{3.6}$. As an aside, it may be mentioned that both hydride phases are too unstable to find wide utility in energy storage applications. However, it is quite likely that related hydrides, produced by modifying the starting alloy composition, will be of interest in this regard. Such modification has proved quite useful in other alloy–hydrogen systems.[3]

Experimental Section

The alloy samples were prepared in an arc furnace from zone-refined titanium and chromium, obtained from the Materials Research Corp., Orangeburg, N.Y., and had reported purities of 99.99%. The sample compositions corresponded to the formula $TiCr_{1.8}$ (66 wt % Cr, 34 wt % Fe), which is in the middle of the homogeneous C15 phase field. Alloys were occasionally prepared from lower grade materials, but no significant change in behavior was noted. Samples were melted six to eight times and normally held in the liquid state for 20–30 s to ensure complete mixing of the starting metals. Then they were visually inspected for the presence of unmelted chromium or titanium by either sawing or cracking them open. Alloys which appeared to be homogeneous were subjected to metallographic and X-ray diffraction analyses as a further check. Each melting of an alloy sample resulted in an average weight loss of ~10 mg causing final maximum deviation from the desired composition of less than 0.5 wt %. Properly melted alloys were then homogenized and annealed. In certain cases, which are noted, as-cast samples were used.

Two slightly different procedures were used to prepare single-phase alloys. The first technique consisted of homogenizing the as-cast buttons by holding them under an inert atmosphere for approximately 5 h at 1370 °C, after which the samples were rapidly quenched by submersion in a water bath. The surfaces of the quenched samples were ground to remove the thin oxide layer caused by the reaction with air and water. Single-phase, β(Cr), solid solutions resulted from this procedure, conforming to the binary Ti–Cr phase diagram shown in Figure 1. The solid solution samples were then annealed in a helium atmosphere at a temperature just below the boundary of the C14–C15 phase transition (~1000 °C) for periods varying from 1 to 2 weeks. After annealing, the samples were allowed to cool slowly to room temperature. The resulting intermetallics were single-phase materials having the C15 structure as determined by micrographic and X-ray diffraction analyses. Electron microprobe analyses were also carried out on a few samples and confirmed the X-ray and micrographic results. The most successful etchant employed for metallurgical preparation of the samples consisted of one part hydrofluoric acid, one part nitric acid, and three parts lactic acid. Final polishing for these materials was achieved by the use of 0.03-μ levigated alumina and fine silk cloth.

The second method employed for obtaining single-phase samples was similar to the first with the exception that the homogenization and subsequent quenching steps were eliminated and annealing times at 1000 °C were extended to 3–4 weeks. This method yielded samples which were single phase as determined by X-ray analysis, but micrographic analysis indicated the presence of a small amount of a second phase. The contaminant phase was thought to be either the high-temperature, C14, phase or a solid solution of variable composition resulting from the severe coring effects which can occur upon initial solidification (see Results and Discussion). However, the amount of the extraneous phase was relatively minor, and these samples can be considered a single phase for our particular purposes. There were no appreciable differences in the pressure–composition isotherms obtained for samples of the same composition prepared by the two different techniques. The first technique, however, is probably preferable since the annealing time is shortened and the resulting alloys were, as far as could be determined, single-phase materials. In both cases, weight loss upon homogenization and annealing was negligible.

The experimental procedure and equipment used to obtain pressure–composition–temperature (P–C–T) relationships in unstable metal–hydrogen systems has been previously described in detail;[4,5] however, for the reader's convenience, a brief synopsis will be given here. All the alloy samples were brittle and were crushed to pass through a 20-mesh screen. The samples, weighing ~10 g, were introduced into a high-pressure reactor which was then sealed and heated under a dynamic vacuum to ~450 °C. In a departure from previous practice, contact with hydrogen at elevated temperatures was avoided as much as possible to prevent possible disproportionation of the intermetallic compound (see Results and Discussion). Then the samples were cooled to room temperature and contacted with hydrogen at pressures up to 70 atm. Upon absorption of some hydrogen, as determined by a decrease in pressure, the samples were further cooled to −78 °C and held at this temperature until no further reaction with hydrogen was observed. During this initial hydriding process, which is commonly referred to as "activation", the alloy particles become highly fractured with a concomitant large increase in surface area. Subsequent reactions with "activated" samples proceed quite rapidly. All the data reported here, unless noted otherwise, were collected with samples that had been subjected to several hydriding–dehydriding cycles.

Pressure–composition relationships were determined in the following manner. A hydrided sample was equilibrated with hydrogen at a pressure of at least 60 atm at a predetermined temperature. An aliquot of hydrogen was then withdrawn from the system by venting to an evacuated reservoir of known volume. After equilibrium was reestablished, as determined by no further pressure change over a period of ~3 h, a further aliquot of hydrogen was withdrawn. This step was repeated in succession until the equilibrium pressure was below 1 atm, after which the sample was quickly heated to ~400 °C and any further hydrogen that evolved was measured. Finally, the reactor was cooled to room temperature, the sample was removed, and any residual hydrogen remaining in the solid was determined by

0020-1669/78/1317-3103$01.00/0

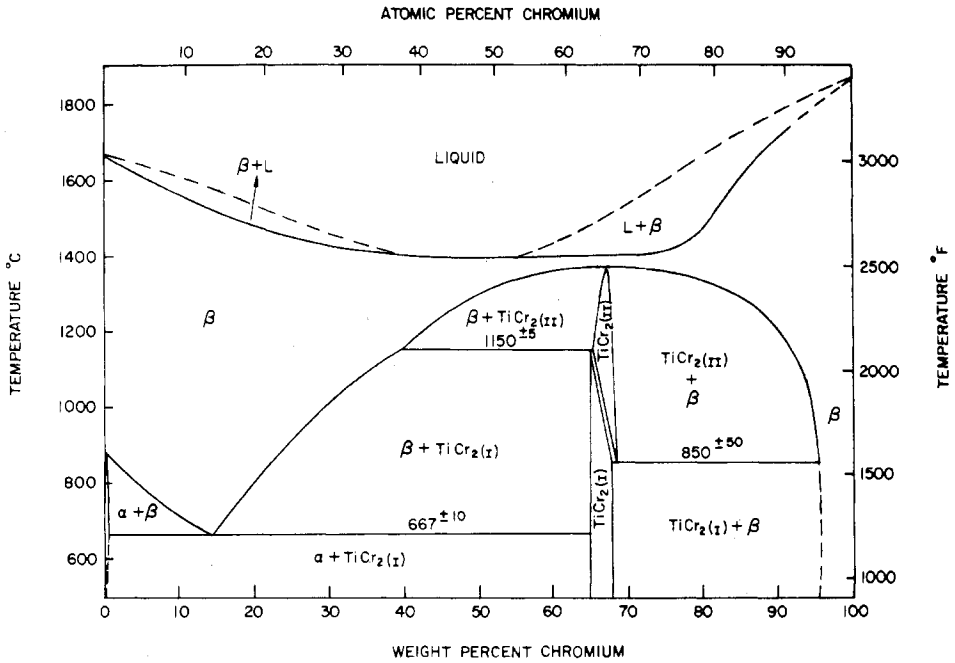

Figure 1. Phase diagram of the Ti–Cr system as determined by Farrar and Margolin.[2]

thermal analysis. The total cumulative error for hydrogen content was estimated to be within ±2.5%. In order to determine hysteresis effects, equilibrium was approached from the opposite direction by adding aliquots of hydrogen to a previously dehydrided, "activated" alloy sample.

All X-ray data were obtained employing Cu or Mo Kα radiation using both a 114.59-mm Norelco powder camera (Debye–Scherrer type) and a Norelco X-ray diffractometer. The starting intermetallics were all crushed, sieved through a 325-standard-mesh screen, reannealed at 1000 °C for a few minutes, and cooled quickly to room temperature before diffraction patterns were obtained. Hydrided samples were stabilized by a special procedure described below.

Unstable hydrides can be deactivated by exposure to air, CO, and other gases.[5] In the present case, hydride samples used for structural determinations were stabilized or deactivated by exposure to liquid CO at −196 °C. The procedure consisted of equilibrating a sample at −78 °C with hydrogen and then injecting high-pressure CO into the reactor. After several hours, the reactor was cooled to −196 °C and evacuated. A further amount of CO was introduced, which condensed, after which the reactor was warmed to room temperature, venting CO as needed to keep the pressure below 60 atm. As a point of safety, it should be emphasized that, during the warming process, caution must be exercised to prevent buildup of excessive pressure by the evaporation of liquid CO (bp −192 °C). At room temperature the CO pressure was reduced to 1 atm and the stabilized hydride was removed from the reactor.

Results and Discussion

The Ti–Cr–H system was investigated using alloys ranging in Cr content from 52.0 to 76.5 wt %. All such alloys reacted with hydrogen to a greater or lesser degree; however primary emphasis was placed on the reaction of hydrogen with $TiCr_2$, a Laves phase having the cubic $MgCu_2$ (C15) structure. This phase is stable at room temperature and is homogeneous between the compositions corresponding to $TiCr_{1.7}$ and $TiCr_{1.9}$. Most of our work was done with alloy compositions in the middle of the phase field, i.e., $TiCr_{1.8}$. A series of pressure–composition isotherms for the $TiCr_{1.8}$–H system is shown in Figure 2. These isotherms are plots of equilibrium dissociation pressure vs. the hydrogen concentration in the solid, expressed as the ratio of the atoms of hydrogen to the total atoms of metal, i.e., H/(Ti + Cr) or simply H/M. The left portion of the graph, where the isotherms rise steeply as a function of hydrogen concentration, is a region of solid solution of hydrogen in the intermetallic compound. This area, by convention, is designated as the α phase of the system. The solubility of hydrogen in the α phase is quite temperature dependent and is relatively large. Upon increasing the hydrogen content of the solid, a region of constant pressure is encountered and the isotherms form a plateau. At −78 °C the inception of the pressure plateau corresponds to an H/M ratio of ~0.4; this composition ($TiCr_{1.8}H_{1.1}$) marks the terminal solubility of hydrogen in the α phase and the precipitation of a hydride phase having the composition $TiCr_{1.8}H_{2.4}$.

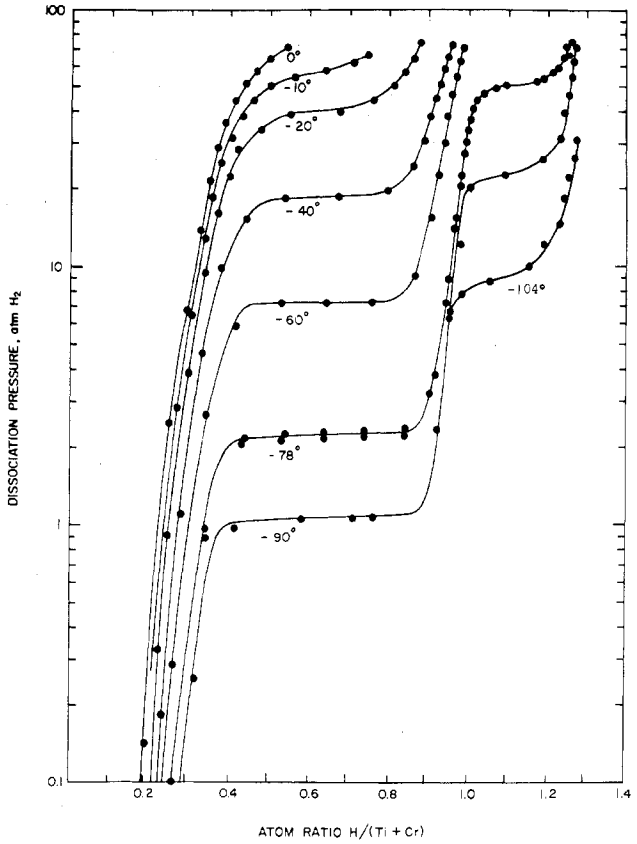

Figure 2. Pressure–composition isotherms for the $TiCr_{1.8}$–H system.

Table I. Relative Partial Molal Quantities per Gram-Atom of Hydrogen at 25 °C

compn	$\bar{H}_H - {}^1/_2H^\circ_{H_2}$, kcal	$\bar{S}_H - {}^1/_2S^\circ_{H_2}$, eu	$\bar{G}_H - {}^1/_2G^\circ_{H_2}$, kcal	A^a	B^a
$TiCr_{1.8}H_{0.84}$	−2.06 ± 0.12	−9.6 ± 0.5	+0.79 ± 0.19	−2077 ± 120	+9.63 ± 0.50
$TiCr_{1.8}H_{1.68}$	−2.41 ± 0.06	−13.2 ± 0.3	+1.53 ± 0.11	−2428 ± 60	+13.32 ± 0.30
$TiCr_{1.8}H_{2.66}$	−2.32 ± 0.17	−14.2 ± 0.8	+1.91 ± 0.29	−2332 ± 170	+14.28 ± 0.80
$TiCr_{1.8}H_{2.94}$	−2.18 ± 0.07	−15.0 ± 0.4	+2.30 ± 0.14	−2195 ± 70	+15.13 ± 0.40
$TiCr_{1.8}H_{3.22}$	−2.04 ± 0.10	−14.4 ± 0.5	+2.24 ± 0.18	−2058 ± 100	+14.49 ± 0.50

[a] Constants in the equation $\ln P_{atm} = (A/T) + B$.

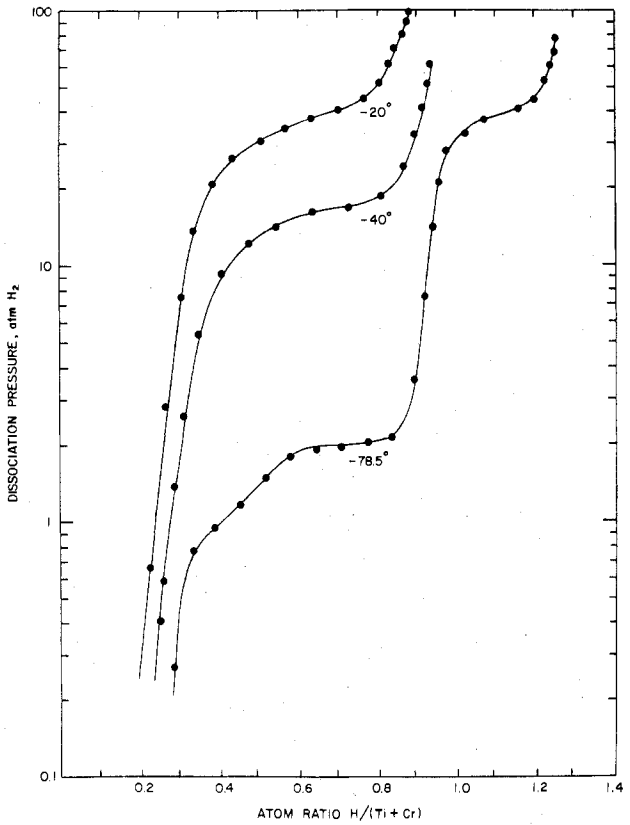

Figure 3. Pressure–composition isotherms for the as-cast $TiCr_{1.8}$–H system.

The plateau persists until the α phase is entirely converted to the hydride phase. It should be noted that the plateau is a consequence of the phase rule, and as the total hydrogen content of the solid increases, only the relative amounts of the two phases change; the hydrogen content of each phase remains constant. When the α phase is entirely converted to the hydride phase, the system regains a degree of freedom and the pressure again rises as the hydrogen concentration in the hydride phase increases. Eventually a second and higher pressure plateau appears which is due to the precipitation of a second hydride phase which has the approximate composition of $TiCr_{1.8}H_{3.4}$ (−78 °C). It will be noted that the limiting compositions of all the phases are temperature dependent.

The phase diagram for the Ti–Cr binary system shows a large temperature difference between the liquidus–solidus curves in the region between 60 and 80 wt % Cr. Consequently, as-cast alloys in this composition region are very inhomogeneous and exhibit severe coring effects. In order to obtain single-phase $TiCr_2$ having the C15 structure, an extensive annealing procedure is required (see above) as the presence of extraneous phases and concentration gradients in as-cast alloys distorts the pressure–composition isotherms. This effect is illustrated in Figure 3, and it should be emphasized that proper sample preparation techniques are required in order to accurately characterize the system, both thermodynamically and structurally.

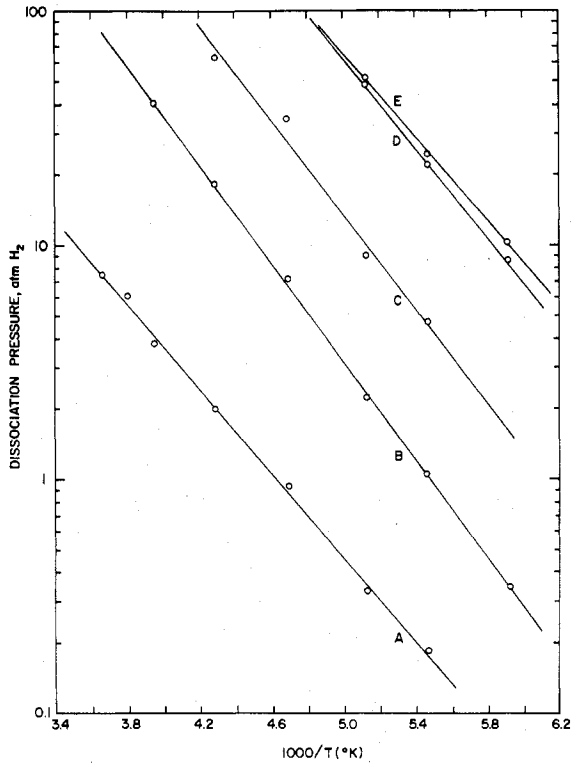

Figure 4. Equilibrium dissociation pressure vs. reciprocal temperature for $TiCr_{1.8}H_x$: (A) $TiCr_{1.8}H_{0.84}$, (B) $TiCr_{1.8}H_{1.68}$, (C) $TiCr_{1.8}H_{2.66}$, (D) $TiCr_{1.8}H_{2.94}$, (E) $TiCr_{1.8}H_{3.22}$.

Starting with the hydrogen-saturated solid, the reactions taking place in the system at −78 °C (Figure 2) may be written

$$1.54TiCr_{1.8}H_{1.1} + H_2 \rightleftarrows 1.54TiCr_{1.8}H_{2.4} \quad (1)$$

which further reacts to form the higher hydride:

$$1.67TiCr_{1.8}H_{2.4} + H_2 \rightleftarrows 1.67TiCr_{1.8}H_{3.6} \quad (2)$$

The product of reaction 2 represents the highest hydrogen content we have so far obtained.

The variation of the ln of the equilibrium dissociation pressure with the reciprocal temperature for several solid compositions is shown in Figure 4. The relationship is linear and obeys the van't Hoff equation in the form of $\ln P_{atm} = (A/T) + B$ where A and B are constants and T is the absolute temperature. Thermodynamic values for the system were derived from these data and are shown in Table I. They are given as relative partial molal quantities ($\bar{X}_H - {}^1/_2X^\circ_{H_2}$) where $\bar{X}_H$ is the partial molal enthalpy (entropy or free energy) of hydrogen (as atoms) in the solid and $X^\circ_{H_2}$ refers to hydrogen in its standard state as a pure, diatomic ideal gas at a pressure of 1 atm.

A most unusual property of this system is that the equilibrium absorption and desorption isotherms almost coincide as illustrated in Figure 5. It will be noted that there is a 1 °C difference between the isotherms and, in the lower plateau region, a pressure difference of 0.2 atm. Upon normalization to a common temperature of −78 °C, this pressure difference

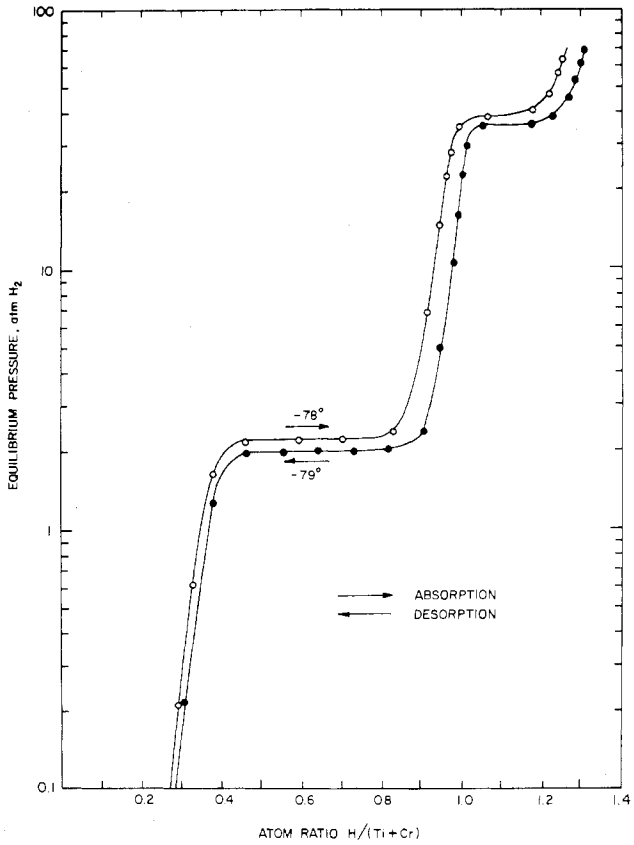

Figure 5. The hysteresis effect in the $TiCr_{1.8}$–H system is notably small. If the desorption data were collected at −78 °C instead of −79 °C, the curves would virtually coincide. (See also Figure 2.)

Table II. Variation of Lattice Parameters (Å) with Hydrogen Content at 25 °C

compn	symmetry	*a*	*b*	*c*
$TiCr_{1.8}$	fccub	6.939		
$TiCr_{1.8}H_{0.30}$	fccub	6.998		
$TiCr_{1.8}H_{0.64}$	fccub	7.017		
$TiCr_{1.8}H_{1.31}$	fccub	7.087		
$TiCr_{1.8}H_{2.58}$	orthorhombic	7.28	5.15	4.95
$TiCr_{1.8}H_{2.91}$	orthorhombic	7.29	5.16	4.93
$TiCr_{1.8}H_{3.42}$	orthorhombic	7.30	5.18	4.94

should be reduced to 0.07 atm which is within the limits of error in our measurements. A similar argument holds for the upper plateau region. The virtual absence of hysteresis in this system is in direct contrast to other unstable metal–hydrogen systems such as TiFe–H_2[5] and $LaNi_5$–H_2[6] and indicates the metal–hydrogen reactions cited above approach true reversibility.

The hydride phases resulting from reactions 1 and 2 are grayish silver, metallike solids which are similar in appearance to the starting intermetallic compound. They are very brittle; they are not pyrophoric upon air exposure but rather tend to become partially deactivated. This deactivation phenomenon has been previously exploited to obtain X-ray diffraction patterns using conventional powder techniques. In the present case, the hydride samples were deactivated by exposure to CO as described above. The X-ray diffraction data indicated the presence of only one miscibility gap at room temperature. These data were combined with the low-temperature *P–C–T* data to construct a phase diagram which is shown in Figure 6. It will be noted that the terminal solubility of hydrogen increases with temperature and at 25 °C corresponds to a composition of $TiCr_{1.8}H_{1.3}$. The lattice parameter of the cubic α phase increases correspondingly as noted in Table II. Only

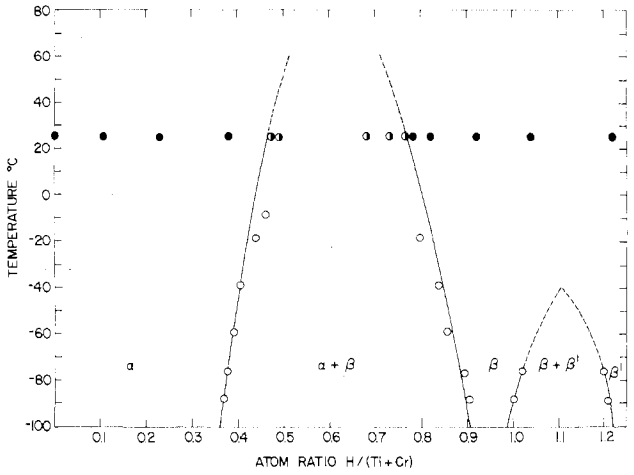

Figure 6. Phase diagram for the $TiCr_{1.8}$–H system derived from *P–C–T* and X-ray diffraction data. The latter were collected at the compositions indicated: ● one solid phase; ◑ two solid phases.

Table III. *d* Spacings for $TiCr_{1.8}H_{3.42}$ at 25 °C[a]

line no.	rel intens	*d*(obsd), Å	*d*(calcd), Å	*hkl*
1	25	2.584	2.591	020
2	75	2.468	2.470	002
3	100	2.203	2.202	310
4	40	2.134	2.133	112
5	33	2.117	2.113	220
6	10	1.823	1.824	400
7	20	1.510	1.501	203
8	8	1.492	1.492	420
9	22	1.406	1.408	330
10	40	1.288	1.296	040
11	10	1.228	1.231	521
12	15	1.106	1.106	423
13	5	1.060	1.056	440
14	12	0.979	0.979	105
15	28	0.953	0.953	350
16	9	0.870	0.871	153
17	7	0.850	0.852	135
18	20	0.821	0.818	505

[a] Orthorhombic; $a = 7.30$ Å, $b = 5.18$ Å, $c = 4.94$ Å.

one hydride phase exists at room temperature, and it has a composition range extending from $TiCr_{1.8}H_{2.1}$ to $TiCr_{1.8}H_{3.6}$. This phase is orthorhombic with the lattice parameters varying slightly with hydrogen content as also shown in Table II. The observed and calculated *d* values for a particular composition are given in Table III.

To our knowledge, this is the first example of a structural transformation of a Laves phase due to hydrogen absorption. Previous investigators[7-9] have noted that a number of ZrM_2 (where M is a transition metal) Laves phases, which absorb large quantities of hydrogen, do not undergo phase transformations but merely lattice expansions. This has also been reported to be the case with $HfV_2H_{1.25}$ which also retains its original C15 structure.[10] However the hydrogen content of the latter compound is rather low; in fact it is below the α, $\alpha + \beta$ phase boundary in the $TiCr_{1.8}$–H system and thus may not be comparable.

The density of deactivated $TiCr_{1.8}H_{2.50}$ as measured under benzene was determined to be 5.08 g/cm^3. This value yielded 3.95 formula units per unit cell using the lattice parameters given in Table II for $TiCr_{1.8}H_{2.58}$.

Upon departing in either direction from the homogeneous $TiCr_2$ phase field, the *P–C–T* isotherms become quite distorted as shown in Figures 7 and 8. The Ti-rich phases form the stable binary TiH_2, as well as the ternary $TiCr_2H_x$. With Cr-rich phases, only the latter hydride forms and, as far as

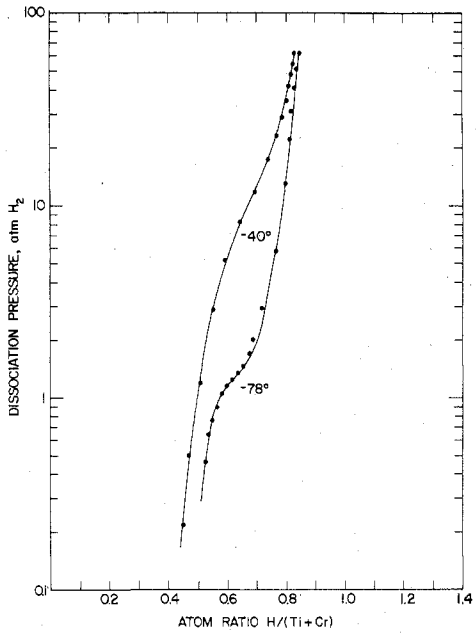

Figure 7. Pressure–composition isotherms for an as-cast Ti-rich alloy having a composition of 47.9 wt % Ti and 52.1 wt % Cr.

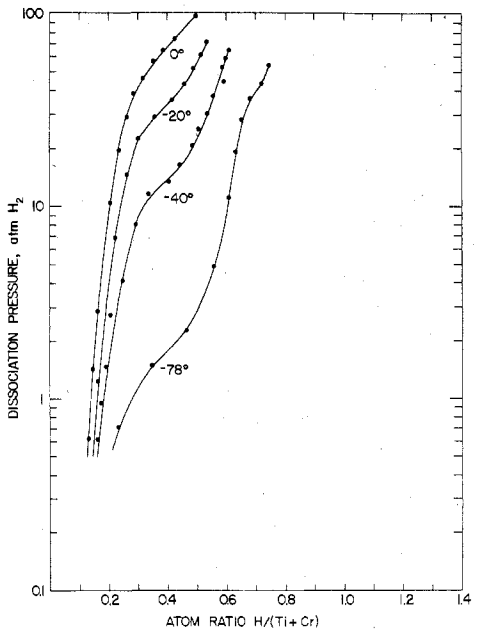

Figure 8. Pressure–composition isotherms for an as-cast Cr-rich alloy having a composition of 23.5 wt % Ti and 76.5 wt % Cr.

could be determined, the β(Cr) solid solution (96 wt % Cr) does not react with hydrogen.

A simple theory has been recently proposed to predict the approximate heat of formation of ternary hydrides from intermetallic compounds.[11] It is based on a model originally devised by Miedema to predict the heat of formation of alloys and intermetallic compounds.[12] The present variation is commonly referred to as the rule of reversed stability, and for a detailed exposition, the reader is referred to the references cited. Here we shall merely note that the model states that the enthalpy (ΔH) of formation of a ternary hydride from an intermetallic compound (not from the elements) is composed of three terms:

$$\Delta H_{AB_nH_{2m}} = \Delta H_{AH_m} + \Delta H_{B_nH_m} - \Delta H_{AB_n} \quad (3)$$

where A and B are metals and A is a stable hydride former. The theory has been quite successful when applied to systems involving the rare earth–transition metal intermetallic compounds. It has been less successful with systems involving Ti alloy hydrides,[13] and the present case is no exception. Consider the following: upon substituting the heats of formation of TiH_2,[14] CrH,[15] and $TiCr_2$ (calculated by Miedema's method), one obtains

$$\begin{aligned}\Delta H_{TiCr_2H_4} &= \Delta H_{TiH_2} + \Delta H_{Cr_2H_2} - \Delta H_{TiCr_2} \quad (4)\\ &= (-30 \text{ kcal}) + (-3.4 \text{ kcal}) - (-3 \text{ kcal})\\ &= -30.4 \text{ kcal or } -15.2 \text{ kcal/mol of } H_2\end{aligned}$$

The above value is too exothermic by about 10 kcal/mol of H_2. The use of stoichiometric compositions, which is the usual practice, does not substantially affect the conclusion.

At this point it seems appropriate to mention a rather important aspect of the reaction of hydrogen with intermetallic compounds or metal alloys. It has been noted that in such reactions the actual path is dependent upon two variables, i.e., the metal atom mobility and the free energy change.[16] At low temperatures the mobility of the metal atoms is very restricted and only martensitic-type phase transformations are possible. In such reactions the metal atoms move only very short distances, although they move in concert. Thus low-temperature reactions will invariably result in the formation of ternary hydride phases which are closely related to the structure of the starting material, even though, in most cases, alternative reactions would be favored from purely free energy considerations. For example, in the present case the following disproportionation reaction is highly favored over the formation of the ternary hydride, i.e., reactions 1 and 2.

$$TiCr_2 + H_2 \rightarrow TiH_2 + 2Cr \qquad \Delta G_{298} = -17.5 \text{ kcal} \quad (5)$$

Of course, at room temperature or below, the above reaction (5) will not occur, at least over any reasonable time span. However at higher temperatures, the mobilities of the metal atoms increase and eventually will be sufficient to permit reaction 5 to proceed as written; i.e., the system will adopt its most stable thermodynamic configuration. It is for this reason we have departed from our previous activation procedure (see above) which includes exposing a virgin alloy sample to hydrogen at temperatures of ~450 °C. More generally it should be assumed that any intermetallic compound of this type will disproportionate in the presence of hydrogen at high temperatures if the free energy change is favorable, and experimental procedures should be revised accordingly.

Acknowledgment. This work was performed under the auspices of the U.S. Department of Energy, Washington, D.C. The authors also wish to thank Drs. F. Reidinger, J. Lynch, and R. H. Wiswall for helpful suggestions, and Messrs. S. Bookless, A. Holtz, and J. Hughes for their help in the laboratory.

Registry No. $TiCr_2$, 12018-27-8; H_2, 1333-74-0; chromium titanium hydride, 65107-39-3.

References and Notes

(1) Reilly, J. J. "Hydrogen: Its Technology and Implications"; Cox, K. E., and Williamson, K. D., Ed.; CRC Press: Cleveland, Ohio, 1977; Vol. II, pp 13–28.
(2) Farrar, P. A.; Margolin, H. *Trans. Metall. Soc. AIME* **1963**, *227*, 1342.
(3) Reilly, J. J.; Johnson, J. R. *Conf. Proc. — World Hydrogen Energy Conf., 1st*, **1976**.
(4) Reilly, J. J.; Wiswall, R. H. *Inorg. Chem.* **1970**, *9*, 1968.
(5) Reilly, J. J.; Wiswall, R. H. *Inorg. Chem.*, **1974**, *13*, 218.
(6) Kuijpers, F. A.; van Mal, H. H. *J. Less-Common Met.*, **1971**, *23*, 395.
(7) Pebler, A.; Gulbransen, E. A. *Electrochem. Technol.* **1966**, *4*(5–6), 211.
(8) Pebler, A.; Gulbransen, E. A. *Trans. Metall. Soc. AIME* **1967**, *239*, 1593.
(9) Shaltiel, D.; Jacob, I.; Davidov, D. *J. Less-Common Met.* **1977**, *53*, 117.
(10) Duffer, P.; Gualtieri, D. M.; Rao, V. U. S. *Phys. Rev. Lett.* **1976**, *37*, 1410.
(11) van Mal, H. H.; Bushow, K. H. J.; Miedema, A. R. *J. Less-Common Met.* **1974**, *35*, 65.
(12) Miedema, A. R.; Boom, R.; DeBoer, F. R. *J. Less-Common Met.* **1975**, *41*, 283.

(13) Yamanaka, K.; Saito, H.; Someno, M. *Nippon Kagaku Kaishi* **1975**, *No. 8*, 1267.
(14) Stalinski, B.; Bieganski, Z. *Bull. Acad. Pol. Sci., Ser. Sci. Chim.* **1960**, *8*, 243.
(15) Wolf, G. Z. *Phys. Chem. (Leipzig)* **1971**, *246*(5/6), 403–406.
(16) Reilly, J. J. "Proceedings of the International Symposium on Hydrides for Energy Storage, Geilo, Norway, 1977"; Pergamon Press: London, in press.

Contribution from the Department of Chemistry,
The University of Texas at Austin, Austin, Texas 78712

A Plasma Synthesis for the Perfluoroalkyl Di-, Tri-, and Tetrasulfides: Reaction of Trifluoromethyl Radicals with Sulfur Vapor

TAKASHI YASUMURA and RICHARD J. LAGOW*[1]

Received April 17, 1978

A new synthesis for a number of perfluoroalkyl di-, tri-, and tetrasulfides ($CF_3S_nCF_3$, $C_2F_5S_nCF_3$, $C_2F_5S_nC_2F_5$, n = 2–4) has been developed using a low-temperature glow discharge to dissociate sulfur vapor and generate trifluoromethyl radicals from hexafluoroethane. These compounds were characterized by mass spectra, infrared spectra, and NMR spectra.

Introduction

Bis(trifluoromethyl) di-, tri-, and tetrasulfides are more stable than their unfluorinated analogues. Previous preparations for these compounds include[2,3]

$$CS_2 + IF_5 \xrightarrow{60\text{–}200\ ^\circ C} CF_3SSCF_3 + SF_4 + CF_3SSSCF_3$$

$$CF_3I + S \xrightarrow[36\ h]{310\ ^\circ C} \underset{(80\%)}{CF_3SSCF_3} + \underset{(7\%)}{CF_3SSSCF_3} + \underset{(1\%)}{CF_3SSSSCF_3}$$

The most often used preparation for bis(trifluoromethyl) disulfide is the reaction of sodium fluoride with thiocarbonyl chloride or trichloromethanesulfenyl chloride in tetramethylene sulfone solution.[4,5]

$$CSCl_2 + NaF \xrightarrow{245\ ^\circ C} CF_3SSCF_3 + CS_2$$

$$CCl_3SCl + NaF \xrightarrow{170\text{–}250\ ^\circ C} CF_3SSCF_3 + CF_3SCl$$

Other similar procedures are[6]

$$Cl_3CSBr + KF \xrightarrow{175\ ^\circ C} CF_3SSCF_3 \quad (68\%)$$

$$Cl_3CSSCCl_3 + KF \xrightarrow{150\text{–}160\ ^\circ C} CF_3SSCF_3 \quad (58\%)$$

We have previously shown that synthetically useful quantities of reactive trifluoromethyl radicals may be obtained from a glow discharge of hexafluoroethane.[7]

Sulfur vapor (mainly S_8) was introduced into the radio-frequency discharge to be dissociated to generate reactive lower molecular weight species:

$$S_n\ (\text{vapor}) \xrightarrow{rf} S + S_2 + S_3 + S_4 + \ldots$$

Through the cocondensation of sulfur vapor and reactive plasma-generated trifluoromethyl radicals, a new route to perfluoroalkyl polysulfides was sought.

Experimental Section

Materials. The sulfur was J. T. Baker sublimed sulfur, N. F. The hexafluoroethane used was Matheson high-purity Freon 116.

A Bendix gas chromatograph equipped with a nickel thermal conductivity detector and a cryogenic temperature controller was used for separations. A 7 m by $^3/_8$ in. column of 10% fluorosilicone on Chromosorb P was used.

Physical Measurements. Infrared spectra of gas-phase products were run in a 10-cm cell with KBr windows using a Beckman IR-20A instrument.

Mass spectra were obtained on a Hitachi RMU-6D mass spectrometer at 70 eV. The species containing sulfur were identified by their isotope patterns.

Fluorine NMR spectra were obtained with a Perkin-Elmer R-20B spectrometer operating at a frequency of 56.47 MHz. Chemical shifts were measured with a Takeda-Riken TR-3824X frequency counter.

Analyses were done by Schwarzkopf Microanalytical Laboratories.

Apparatus. The radio-frequency power source was a Tegal Corp. Model RF6100 100-W, 13.56-MHz radio-frequency generator with a matching network operating at approximately 20 W.

The apparatus in which the syntheses were carried out is shown in Figure 1.

Hastings thermocouple vacuum gauges (A), Model DV-5M or Model DV-4DM, were used to monitor the system pressure. A Viton O-ring junction (B) connected the two plates of two Pyrex glass reactors.

The helical coil (C) consists of six turns of $^3/_{16}$-in. copper tubing and is connected to the radio-frequency oscillator.

The C_2F_6 was introduced at the inlet (D) of the reactor. The solid sulfur was heated to the desired temperature using a mantle heater. The two Pyrex traps (E) before the vacuum pump were cooled using liquid nitrogen.

General Procedure. Sulfur powder was placed in the bottom of the reaction chamber. A liquid-nitogen trap was placed before the pump, and the system was evacuated to less than 5 mTorr.

The sulfur powder was heated to the desired temperature (>165 °C) and C_2F_6 was introduced into the reactor. The system pressure, which was equal to the C_2F_6 pressure (the sulfur vapor condensed rapidly), was measured by a thermocouple vacuum gauge. A Dewar containing liquid nitrogen was put around the product trap. The blue-colored plasma was then initiated.

After the reaction, the system pressure was measured.

Slush baths of various temperatures were used for low-temperature vacuum fractionation. Each product from each fractionation was then examined by IR spectroscopy. Further GC separations were then carried out. The pure products separated by GC were examined by infrared spectroscopy, mass spectroscopy, NMR spectroscopy, and elemental analysis.

Reaction of Sulfur Vapor with Trifluoromethyl Radicals

Sulfur powder was heated to the liquid state at ca. 165 °C. (The temperature was estimated without the plasma under the same conditions as were used during the reaction.) C_2F_6 at a pressure of 100 mTorr was introduced into the reactor from the C_2F_6 inlet tube in front of the radio-frequency coil. After a 6 h run, the contents in the liquid-nitrogen trap were fractionated at −35.6, −78, and −131 °C, and each fraction was further separated by gas chromatography. The −131 °C fraction contained C_2F_6. The −35.6 and −78 °C fractions were separated by GC at a column temperature of 30 °C.

0020-1669/78/1317-3108$01.00/0